능동 및 수동격리기를 적용한 진동계에 있어서 힘의 전달에 관한 연구

이진우[†] · Colin H. Hansen[*]
한국산업안전공단 부산지역본부 · 호주아델라이드대학교 기계공학과
(2001. 2. 27. 접수 / 2001. 11. 20. 채택)

Power Transmission from a Vibrating Mass to a Supporting Plate through Isolators

Jin-Woo Lee[†] · Colin H. Hansen[*]
Technical Experts Team, Korea Occupational Safety and Health Agency, Pusan, Korea
[*]Department of Mechanical Engineering, University of Adelaide, South Australia 5005, Australia
(Received February 27, 2001 / Accepted November 20, 2001)

Abstract : The transmission of harmonic vibratory power from a vibrating rigid body into a supporting plate through passive and active isolators is investigated theoretically and experimentally. The theoretical model allows for the transmission of vertical and horizontal harmonic forces and moments about all three coordinate axes. The experiment is to use vibration actuators attached to the intermediate mass of the two-stage mount to minimize the rotational and translational vibration of the intermediate mass. The performance is done by measuring the vibration at the error sensors due to the primary vibration source and measuring the transfer functions from the control sources to the error sensors. Results show that over a frequence range from 1 to 100Hz, transmission into the supporting plate can be reduced substantially by employing in parallel with existing passive isolators, active isolators adjusted to provide appropriate control force amplitudes.

요 약 : 회전하는 기계에서 전달되는 조화적인 진동력이 수동 및 능동 진동 격리기를 통하여 중간 지지구조물에 어떻게 전달되는 것인가를 연구하였다. 이를 위하여 이론적인 모델은 모든 축에 대하여 수평과 수직방향의 힘과 모멘트를 고려하여 작성되었으며, 실험은 중간 구조물에 전달되는 회전방향 및 직선방향의 진동을 최소화하기 위하여 2단으로 구성된 중간 지지구조물에 부착된 진동 액츄에이터를 사용하였다. 진동원에 의하여 발생된 진동이 에러 센서에서 측정되었으며 제어원과 에러센서사이의 전달함수가 측정되었다. 1~100Hz 사이의 주파수 범위에 있어서 기존의 수동격리기와 직렬로 설치된 능동격리기를 통하여 전달된 힘이 실제로 감소되었음을 실험결과를 통하여 확인하였다.
Key Words : active vibration control, control shaker, error sensor

1. Introduction

Conventional passive vibration isolation of machinery from supporting structures, typically utilizes springs, air mounts, rubber blocks or sheets of neoprene. An isolation system is usually selected based on the operating frequency of the machine. For example, an electric motor rotating at 1440rpm has an operating frequency of 24Hz. The machine mounted on the vibration isolators must have a resonance frequency less than the driving frequency for vibration isolation to occur. More specifically, the driving frequency of the machine should be at least $\sqrt{2}$ times the resonance frequency of the system. However, by selecting a vibration isolator of low stiffness, so that greater isolation occurs, the deflection of the mount will be large and this may result in unacceptable instability of the system. One way of addressing these constraints is to replace the passive

[†]To Whom Correspondence should be addressed.
ljw601@kosha.net

isolation system with an entirely active system. A preferred option is to add an active vibration control element in parallel or series with conventional passive vibration mounts. One disadvantage is that the active system may transmit vibration that generates unwanted vibration such as high frequency vibration or forces and moments that act to increase the vibration in support structure.[1]

When considering the possibility of including a feed-forward adaptive isolation system in parallel with existing passive equipment isolators for minimizing harmonic vibratory power transmission from vibrating equipment to a supporting structure, it is useful to have an analytical model to estimate potential performance benefits.[2,3] A review of previous work[4,5] considers the general topic of active vibration isolation.

The purpose of the work described here is to develop such a model which allows the calculation of the harmonic vibratory power transmission from an arbitrarily vibrating rigid body to a supporting plate.

And it is to demonstrate the feasibility of using active vibration control to reduce low frequency vibration transmission through an existing passive isolation system. The work involved the use of a feedforward controller to minimize the motion of the intermediate mass (assumed rigid) of a two-stage mount so that the vibratory energy transmitted to the support structure could be minimized. To do this, the error signals for the controller were obtained using accelerometers mounted on the intermediate mass and the cost function to be minimized was the sum of the squared error signals, which is equivalent to minimizing the kinetic energy of the intermediate mass.

2. Theoretical Mode

A. Rigid body equation of motion

The experimental rig is modelled as a six- degree-of-freedom rigid body which is supported by a flexible rectangular plate through multiple elastic mounts, as shown in Fig. 1. A vibratory source of frequency ω acting on the rigid body can be described by a harmonic external force vector $[Q_0]e^{j\omega t}$ acting on the center of gravity of the body as follows[7,8]:

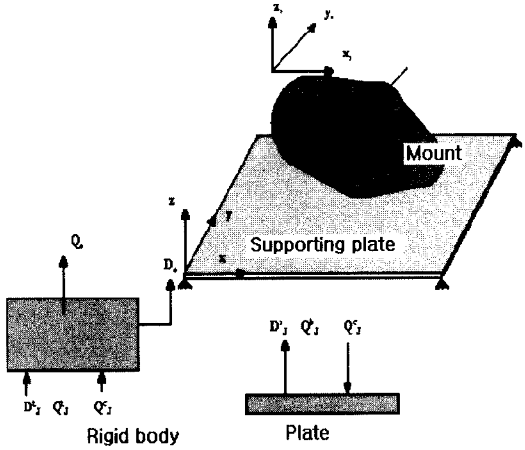

Fig. 1. Rigid body isolated from a supporting plate by multiple isolation mounts

$$[Q_0]=[F_x\ F_y\ F_z\ M_x\ M_y\ M_z]^T \tag{1}$$

where the symbols F and M are, respectively, the force and moment components of the 6-D force vector.

Referring to Fig. 1 the equation of motion of the rigid body at the harmonic frequency ω can be written as[9]

$$Z_0D_0 = Q_0 + \sum_{j=1}^{L_1} R_j^t Q_j^t \tag{2}$$

where D_0 is the complex displacement matrix of the centre of gravity of the rigid body, $Q^t{}_j$ is the force coupling matrix at top of jth isolator, L_1 is the number of isolators, $R^t{}_j$ is the matrix which accounts for coupling between moments and translational displacements and $Z_0=-\omega^2 m_0$, ω is the primary force excitation frequency and m_0 is the diagonal inertia matrix.

B. Supporting plate equation of motion

By considering the force(in the z-direction) and moments(around the x- and y-axes) equilibrium, by including the influence of the external forces and by modelling the mass loading m_j^b of each mount on the supporting plate at frequency ω as a concentrated inertial force $m_j{}^b\omega^2 w(\sigma,\omega)\delta(\sigma-\sigma_j)$, the plate displacement, $w=w(\sigma,\omega)$ can be described by the following partial differential equation[9]:

$$\rho h\frac{\partial^2 w}{\partial t^2}+\frac{Eh^3}{12(1-\upsilon^2)}\nabla^4 w=\sum_{j=1}^{L_1}[F^b_{zj}\delta(\sigma-\sigma_j) + \frac{hF^b_{xj}}{2}\frac{\partial\delta(\sigma-\sigma_j)}{\partial x}+\frac{hF^b_{yj}}{2}\frac{\partial\delta(\sigma-\sigma_j)}{\partial x} - M^b_{xj}\frac{\partial\delta(\sigma-\sigma_j)}{\partial y}+M^b_{yj}\frac{\partial\delta(\sigma-\sigma_j)}{\partial x} + m^b_j\omega^2 w(\sigma,\omega)\delta(\sigma-\sigma_j)] \quad (3)$$

where ρ, E, υ and h are the density, Young's modulus of elasticity, Poisson's ratio and thickness respectively of the plate. The quantity $\sigma_j=(x_j, y_j)$ is the location vector of the jth mount on supporting plate surface, and $\delta(\sigma-\sigma_j)$ is the Dirac delta function.

Using modal analysis, the plate displacement $w(\sigma,\omega)$ can be expressed in terms of mode shape matrix $\psi_p(\sigma)=[\psi_1(\sigma),\psi_2(\sigma),\cdots,\psi_P(\sigma)]^T$ and a modal amplitude coefficient matrix $w_p(\sigma)=[w_1, w_2,\cdots,w_P]^T$ as:

$$w=w(\sigma,\omega)=\psi_p^T(\psi)w_p \quad (4)$$

where $\psi_I^T(\sigma)$ is I th plate mode shape function of a simply supported rectangular plate.

Substituting (4) into (3) and using the orthogonal property of the mode shape functions and Dirac delta functions, the coefficient w_I for Ith plate mode becomes:

$$m_I(\omega_I^2+j\eta_I\omega^2)w_I=\sum_{j=1}^{L_1}\left[\frac{h}{2}\psi_{Ix}(\sigma_j), -\frac{h}{2}\psi_{Iy}(\sigma_j),\psi_I(\sigma_j), -\psi_{Iy}(\sigma_j),\psi_{Ix}(\sigma_j),0\right] Q^t_j+\sum_{I'=1}^{P}C_{I',I}w_{I'} \quad (I=1,2,\cdots,P) \quad (5)$$

where m_I, ω_I, η_I and $C_{I',I}$ are the modal masses, the angular resonance frequency of the Ith plate mode, the loss factor of the Ith plate mode and the concentrated mass contribution respectively.

When I in (5) increments from 1 to P, P simultaneous equations can be obtained for the coefficients $w_1, w_2,\cdots,w_P$, and the matrix equation for w_P is obtained as:

$$Z_P w_P=\sum_{j=1}^{L_1}R^b_j Q^b_j \quad (6)$$

where Z_P is the uncoupled plate characteristic matrix including influence of the concentrated masses of the mounts and the quantity R^b_j is the force coupling matrix for the jth mount.

C. System equations of motion

The matrix relation for displacements at the bottom of the mount is

$$D^b_j=(R^b_j)^T w_p \quad (7)$$

where $R^b{}_j$ is the force coupling matrix on supporting plate for the jth mount.

A matrix equation describing the response of the coupled system can be obtained as follows:

$$\begin{bmatrix}A_{11} & A_{12}\\ A_{21} & A_{22}\end{bmatrix}\begin{bmatrix}D_0\\ w_p\end{bmatrix}=\begin{bmatrix}Q_0\\ 0\end{bmatrix} \quad (8)$$

where D_0 is displacement vector of rigid body, Q_0 is harmonic driving force vector and the element matrices $A_{11},\cdots,A_{22}$ are given by the following expressions:

$$A_{11}=Z_0+\sum_{j=1}^{L_1}R^t_jK_j(R^t_j)^T \quad (9a)$$

$$A_{12}=-\sum_{j=1}^{L_1}R^t_jK_j(R^b_j)^T \quad (9b)$$

$$A_{21}=-\sum_{j=1}^{L_1}R^b_jK_j(R^t_j)^T \quad (9c)$$

$$A_{22}=Z_p+\sum_{j=1}^{L_1}R^b_jK_j(R^b_j)^T \quad (9d)$$

The resonance frequencies and mode shapes of the coupled system can be obtained by solving the eigenvalue problem of the coefficient matrix $[A]$ when $[Q_0]=0$:

$$[A]=\begin{bmatrix}A_{11} & A_{12}\\ A_{21} & A_{22}\end{bmatrix} \quad (10)$$

D. Active isolator

A passive isolator can be made active by introducing a force actuator connected in parallel with it. When used with a suitable feedforward control system, the actuator exerts a control force on the rigid body and the support point on the panel simultaneously. For active isolators acting at the same location as the passive isolators, the right part of Eq. (8) is replaced by a combined force vector, and the equation of motion becomes:

$$\begin{bmatrix} A_{11} & A_{12} \\ A_{21} & A_{22} \end{bmatrix}\begin{bmatrix} D_0 \\ w_p \end{bmatrix} = \begin{bmatrix} Q_0 + \sum_{j=1}^{L_1} R_j^t Q_j^c \\ -\sum_{j=1}^{L_1} R_j^b Q_j^c \end{bmatrix} \tag{11}$$

where Q_j^c are the control force vectors generated by each actuator acting on the support panel.

E. Power transmission into the support plate

The cost function chosen for minimization is the time average power transmission into the supporting plate through the isolators, and can be expressed as follows:

$$P_0 = \mathrm{Re}\left\{-\frac{1}{2} j\omega \sum_{j=1}^{L_1} (Q_j^b - Q_j^c)^H D_j^b\right\} \tag{12a}$$

$$= \frac{\omega}{2}\ \mathrm{Im}\left\{\sum_{j=1}^{L_1} (Q_j^b - Q_j^c)^H D_j^b\right\} \tag{12b}$$

$$= \frac{\omega}{2}\,\mathrm{Im}\left\{\sum_{j=1}^{L_1} (D_j^b)^H (Q_j^b - Q_j^c)\right\} \tag{12c}$$

where superscript H represents the transpose and conjugate of a matrix. In case where the matrix is real, H can be replaced with symbol T representing the transpose of the matrix. The time average power transmission from the rigid body into the isolators can be described as:

$$P_t = \mathrm{Re}\left\{-\frac{1}{2} j\omega \sum_{j=1}^{L_1} (Q_j^t + Q_j^c)^H D_j^t\right\} \tag{13}$$

and the input power due to the external driving force is given by:

$$P_i = \mathrm{Re}\left\{-\frac{1}{2} j\omega Q_0^T D_0\right\} \tag{14}$$

It is possible to express the total output power P0 by using an explicit quadratic function. Thus, the term $\sum_{j=1}^{L_1} (D_j^b)^H (Q_j^b - Q_j^c)$ in Eq. (12c) can be expressed as:

$$\sum_{j=1}^{L_1} (D_j^b)^H (Q_j^b - Q_j^c) = (Q^c)^H a Q^c + (Q^c)^H b_1 + b_2 Q^c + c \tag{15}$$

where $Q^c = [Q_1^c, Q_2^c, \cdots, Q_j^c]^T$.

The form of the matrices a, b_1, b_2 and c is dependent on the number of isolators used and to make the solution of this problem tractable, we will consider only four isolators between the rigid body and the support plate; that is, L_1=4. In this case, the matrices a, b_1, b_2 and c may be defined as follows:

$$\sum_{j=1}^{4} (D_j^b)^H (Q_j^b - Q_j^c) = (Q^c)^H a Q^c + (Q^c)^H b_1 + b_2 Q^c + c \tag{16}$$

where

$$a = G_1 K G_2 - G_1 \tag{17}$$

$$b_1 = G_1 K G_3 \tag{18}$$

$$b_2 = G_4 K G_2 - G_4 \tag{19}$$

$$c = G_4 K G_3 \tag{20}$$

and

$$G_1 = \begin{bmatrix} H_1^H R_1^b & H_1^H R_2^b & H_1^H R_3^b & H_1^H R_4^b \\ H_2^H R_1^b & H_2^H R_2^b & H_2^H R_3^b & H_2^H R_4^b \\ H_3^H R_1^b & H_3^H R_2^b & H_3^H R_3^b & H_3^H R_4^b \\ H_4^H R_1^b & H_4^H R_2^b & H_4^H R_3^b & H_4^H R_4^b \end{bmatrix} \tag{21}$$

$$G_2 = \begin{bmatrix} (R_1^t)^T H_5 - (R_1^b)^T H_1 & (R_1^t)^T H_6 - (R_1^b)^T H_2 & (R_1^t)^T H_7 - (R_1^b)^T H_3 & (R_1^t)^T H_8 - (R_1^b)^T H_4 \\ (R_2^t)^T H_5 - (R_2^b)^T H_1 & (R_2^t)^T H_6 - (R_2^b)^T H_2 & (R_2^t)^T H_7 - (R_2^b)^T H_3 & (R_2^t)^T H_8 - (R_2^b)^T H_4 \\ (R_3^t)^T H_5 - (R_3^b)^T H_1 & (R_3^t)^T H_6 - (R_3^b)^T H_2 & (R_3^t)^T H_7 - (R_3^b)^T H_3 & (R_3^t)^T H_8 - (R_3^b)^T H_4 \\ (R_4^t)^T H_5 - (R_4^b)^T H_1 & (R_4^t)^T H_6 - (R_4^b)^T H_2 & (R_4^t)^T H_7 - (R_4^b)^T H_3 & (R_4^t)^T H_8 - (R_4^b)^T H_4 \end{bmatrix} \tag{22}$$

$$G_3 = \begin{bmatrix} (R_1^t)^T B_{11} - (R_1^b)^T B_{21} \\ (R_2^t)^T B_{11} - (R_2^b)^T B_{21} \\ (R_3^t)^T B_{11} - (R_3^b)^T B_{21} \\ (R_4^t)^T B_{11} - (R_4^b)^T B_{21} \end{bmatrix} [Q_0] \tag{23}$$

$$G_4 = Q_0^T[B_{21}^H R_1^b \; B_{21}^H R_2^b \; B_{21}^H R_3^b \; B_{21}^H R_4^b] \quad (24)$$

$$K = \begin{bmatrix} K_1 & & & \\ & K_2 & & \\ & & K_3 & \\ & & & K_4 \end{bmatrix} \quad (25)$$

where matrices H_1 - H_8 are defined as follows:

$$H_1 = B_{21}R_1^t - B_{22}R_1^b \quad (26a)$$

$$H_2 = B_{21}R_2^t - B_{22}R_2^b \quad (26b)$$

$$H_3 = B_{21}R_3^t - B_{22}R_3^b \quad (26c)$$

$$H_4 = B_{21}R_4^t - B_{22}R_4^b \quad (26d)$$

$$H_5 = B_{11}R_1^t - B_{12}R_1^b \quad (26e)$$

$$H_6 = B_{11}R_2^t - B_{12}R_2^b \quad (26f)$$

$$H_7 = B_{11}R_3^t - B_{12}R_3^b \quad (26g)$$

$$H_8 = B_{11}R_4^t - B_{12}R_4^b \quad (26h)$$

and the matrices B_{11}, B_{12}, B_{21}, B_{22}, in the above expressions are the submatrix elements of the inverse of system matrix A, as follows:

$$\begin{bmatrix} B_{11} & B_{12} \\ B_{21} & B_{22} \end{bmatrix} = \begin{bmatrix} A_{11} & A_{12} \\ A_{21} & A_{22} \end{bmatrix}^{-1} \quad (27)$$

$$B_{11} = [A_{11} - A_{12}A_{22}^{-1}A_{21}]^{-1} \quad (28)$$

$$B_{22} = [A_{22} - A_{21}A_{11}^{-1}A_{12}]^{-1} \quad (29)$$

$$B_{12} = -A_{11}^{-1}A_{12}[A_{22} - A_{21}A_{11}^{-1}A_{12}]^{-1} \quad (30)$$

$$B_{21} = -A_{22}^{-1}A_{21}[A_{11} - A_{12}A_{22}^{-1}A_{21}]^{-1} \quad (31)$$

The control force vector Q^c of dimension(24×1) in Eq.(16) is a combined vector of control forces as follows:

$$Q^c = [Q_1^c \; Q_2^c \; Q_3^c \; Q_4^c]^T \quad (32)$$

Thus, by evaluating Eq.(12) and grouping the imaginary terms, the total time average output power P_0 can be expressed as the following real quadratic function, with a symmetrical coefficient matrix for the quadratic term:

$$P_0 = -\frac{\omega}{2}\{(q^c)^T \alpha q^c + (q^c)^T \beta + \beta^T q^c + c^i\} \quad (33)$$

where

$$\alpha = \alpha^T = \frac{1}{2}\begin{bmatrix} a^i + (a^i)^T & a^r - (a^r)^T \\ -a^r + (a^r)^T & a^i + (a^i)^T \end{bmatrix} \quad (34)$$

$$\beta = \frac{1}{2}\begin{bmatrix} (b_2^i)^T + b_1^i \\ (b_2^r)^T - b_1^r \end{bmatrix} \quad (35)$$

and

$$q^c = [Q^{cr} \; Q^{ci}]^T \quad (36)$$

Clearly, the real output power for the uncontrolled case where $q^c=0$ is given by

$$P_0{}' = -\frac{1}{2}\omega c^i \quad (37)$$

A reduction of output power as a result of the action of the control forces will occur when the relationship $\triangle P = P_0{}' - P_0 < 0$ is satisfied. In other words, control force vectors satisfying inequality can result in a reduction of the output power:

$$(q^c)^T \alpha q^c + (q^c)^T \beta + \beta^T q^c < 0 \quad (38)$$

We know that the quadratic function of Eq.(33) has a minimum given by

$$P_{\min} = \frac{\omega}{2}\{\beta^T \alpha^{-1} \beta - c^i\} \quad (39)$$

corresponding to an optimum control force vector of

$$q_{opt}^c = -\alpha^{-1}\beta \quad (40)$$

where the coefficient matrix α is a positive definite matrix.

The quantity P_{min} is theoretically equal to zero for an ideal controller, but the preceding analysis allows the characteristics of a non-ideal controller to be taken into account.

3. Experiment

A. Instrumentation setup

In the figure 2, for the passive system, the top mass is connected to the intermediate mass through 4 rubber isolators and another 6 isolators were mounted between the intermediate mass and the bottom mass. The masses of the top mass, intermediate mass and bottom mass are 54.9kg, 481.3kg and 71kg, respectively. The intermediate mass, measuring 700L×510W×170H, was mounted between the upper mass and the base structure. Seven accelerometers consisted of four at vertical direction and two in the y- and one in the x- direction, were connected to charge amplifiers, which were in turn connected to a digital signal analyzer. They were used to measure the approximate kinetic energy (KE) of the vibration isolator before and after the application of active control.

The active vibration control system used seven accelerometers for the error sensors and seven inertial shakers as control sources, all of which were located on the intermediate mass. To control the transverse motion, pitch and rotation of the mass, four error sensors and four control shakers were mounted on the top of the intermediate mass. Two error sensors and two control shakers were mounted on one side of the mass and one error sensor and one control shaker were mounted on the adjacent side so that rotational motion about the Z axis and the two translational motions in the XY plane could be controlled. Seven monitor sensors were used to evaluate the simulated control results. The distribution of the control shakers, error sensors and monitor sensors are shown in Figure 3.

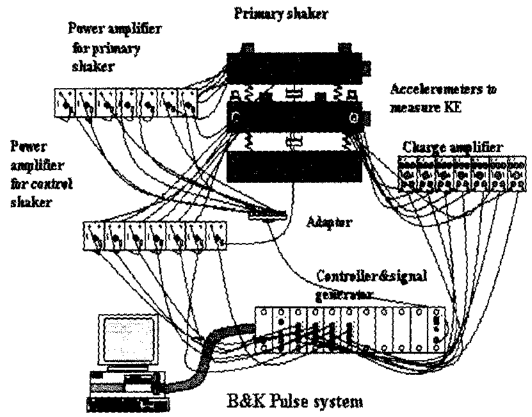

Fig. 2. Instrumentation set up for experimental demonstration

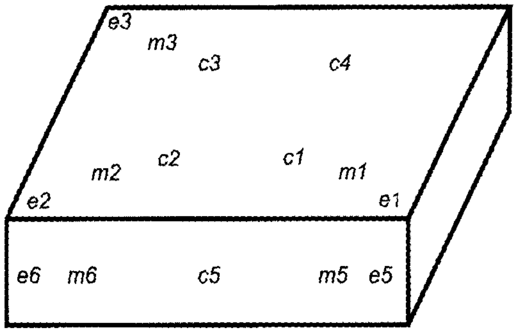

Fig. 3. Error sensor, monitor sensor and control shaker locations

In the figure, c1-c7 are the control shaker locations, and e1-e7 and m1-m7 are the error sensor and monitor locations respectively.

Here, feedforward active vibration control was used, for which a digital controller generated an appropriate control signal based on the error and reference signals. The controller used an adaptive FIR filter,[9] which had the objective of minimizing the error signal. To do this, a Causal Systems EZ-ANC II digital feedforward controller was used to generate the control signals for the control shakers. The signal for driving the primary vibration was fed into the controller as a reference signal.

To simulate the disturbance vibration, seven inertial shakers were mounted to the top mass. Four were mounted with their axes in the Z direction, one with its axis

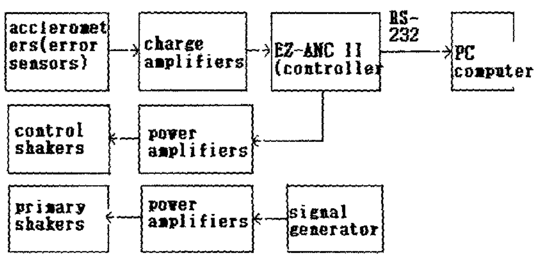

Fig. 4. Block diagram of the experimental setup

in the Y direction, and two with their axes in the X direction.

To maximize the mechanical output of the shakers (control and primary) at the frequency of interest, the resonance frequencies of the control shakers were tuned to match the primary excitation frequency. A block diagram of the experimental setup is shown in Fig. 4.

B. Results and Discussion

Prior to using the EZ-ANC II controller to generate the control signals, it was decided to determine the maximum control that could be achieved using an ideal controller. This work involved measurement of the primary disturbance and measurement of the transfer functions between the control sources and error sensors, mounted as shown in Figure 3. A similar method has been used in the past by others.[10] An experiment was carried out using an EZ ANC-II controller. Seven control shakers and seven error sensors were used, and the cost function that was minimized was the sum of the squared error signals at the error sensors. The signals from the error sensors were input to the EZ ANC-II controller and also to a Brüel & Kjær PULSE system. The average reduction of the sum of the squared signals at the error sensors was then measured using the PULSE system. Control adaptation ceased once this reduction reached a maximum. The power spectra at the error sensors were then recorded.

The vibration isolation performance was determined by summing the squared acceleration of 7 accelerometers mounted on the intermediate mass

Fig. 5 shows the acceleration level reduction in overall performance of the active vibration control with the existing passive isolators. According to the primary disturbance simulated with primary shakers as rotation of 1440RPM, strong vibrations were generated at 24Hz, 36Hz and 48Hz over a low frequency range from 1 to 100Hz. From the figure, as expected, it can be seen that overall acceleration level reduction was approximately 14dB, but the largest reduction at error sensor location was 38dB at 24Hz. Although acceleration level at several point did increase compared with passive vibration isolation, one can see that in this case study all the acceleration level increases occurs at sensing locations where primary shakers are every low.

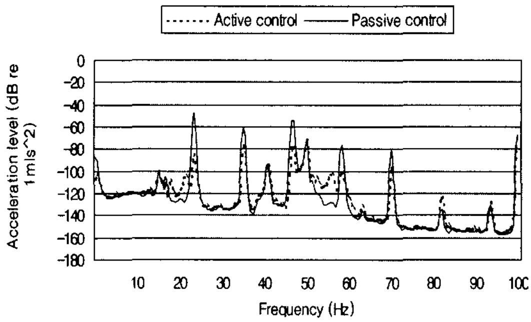

Fig. 5. Comparison between the passive and active control

4. Conclusion and Future Work

The work described here is to presented an analytical model to calculate the maximum achievable reduction of vibratory power transmission from a rigid body through passive and active isolators to a supporting plate. To do this, the cost function which was minimized was the sum of the squared accelerations at the error sensors, which is proportional to the total vibratory energy contained in all six degrees of freedom of the rigid intermediate mass.

According to experimental result we can know that it is possible to significantly reduce the vibratory energy transmission from an intermediate mass to a receiver structure by means of active vibration control. The total vibratory energy of interest frequency could be experimentally reduced by 14dB. And It was found that when the driving force is aligned with the vibration isolators, it is theoretically possible to reduce the vibratory power transmission into the supporting plate to zero. However, when the driving force is not aligned with the axes of the vibration isolators, active control provides limited vibration attenuation. Future work will be conducted investigation for feasibility of using active control to prevent major industrial accident caused by vibration of rotating machine in chemical plant such as pumps, reciprocating compressor, turbine and blower, which will be evaluated the result between the simulated and measured data.

Acknowledgments : The author gratefully acknowledges Financial support for this work from Korean Science and Engineering Foundation and Korea Occupational Safety and Health Agency.

References

1) B. A. T. Petersson. "Moment and force excitation at edges and corners of beam and plate like structures," In International Conference on Recent Advances in structural Dynamics, ISVR, South hampton, pp. 148~157, 1991.
2) Pan, J.-Q. and Hansen, C. H., "Active control of power flow from a vibrating rigid body to a flexible panel through two active isolators," Journal of the Acoustical Society of America, 93, pp. 1947~1953, 1993.
3) Y. K. Koh and R. G. White. "Analysis and control of vibrational power transmission to machinery supporting structures subjected to a multi-excitation system," Parts I-III. Journal of Sound and Vibration, 196(4): pp. 469~522, 1996.
4) Pan, J .Q., Hansen C. H. and Pan, J. "Active isolation of a vibration source from a thin beam using a single active mount," Journal of the Acoustical Society of America, 94, pp. 1425~1434, 1993.
5) C. Q. Howard and C. H. Hansen. "Finite element analysis of active vibration isolation using vibrational power as a cost function," International Journal of Acoustics and Vibration, 4(1): pp. 23~36, 1999.
6) Pan, J., Ming, R., Hansen, C. H. and Clark, R. L., "Experimental determination of the total vibratory power transmission into an elastic beam," Journal of the Acoustical Society of America, 103, pp. 1673~1676, 1998.
7) Howard, C. Q. Hansen C. H, and Pan J. Q, "Power transmission from a vibrating body to a circular cylindrical shell through passive and active isolators," J. Acoust. Soc. Am., 101(3), pp. 1479~1491, 1997.
8) C. Q. Howard. "Active isolation of machinery vibration from flexible structures," Ph.D thesis, University of Adelaide, Australia, 1999.
9) C. H. Hansen and S. D. Snyder. Active Control of Noise and Vibration. E & FN Spon, London UK.
10) C. M. Dorling, G. P. Eatwell, S. M. Hutchins, C. F. Ross, and S. G. C. Sutcliffe. "A demonstration of active noise reduction in an aircraft," Journal of Sound and Vibration. 112(2): pp. 389~395, 1987.